

Magnetoconductivity oscillations induced by intersubband excitation in a degenerate 2D electron gas

Yu.P. Monarkha^{1,*}

¹*B. Verkin Institute for Low Temperature Physics and Engineering, 47 Nauky Ave., 61103, Kharkiv, Ukraine*

Magnetoconductivity oscillations and absolute negative conductivity induced by nonequilibrium populations of excited subbands in a degenerate multisubband two-dimensional electron system are studied theoretically. The displacement from equilibrium, which can be caused by resonant microwave excitation or by any other reason, is assumed to be such that electron distributions can no longer be described by a single Fermi level. In this case, in addition to the well-known conductivity peaks occurring at the Shubnikov-de Haas conditions and small peaks of normal intersubband scattering, sign-changing oscillations with a different shape are shown to be possible. We found also that even a small fraction of electrons transferred to the excited subband can lead to negative conductivity effects.

PACS numbers: 73.40.-c, 75.47.-m, 73.50.-h, 73.50.Pz, 73.63.Hs

I. INTRODUCTION

The transport properties of a 2D electron gas in a perpendicular magnetic field have attracted much interest^{1,2} because of unexpected discoveries and new physics. In addition to the amazing quantum Hall effects observed in a degenerate 2D electron gas under equilibrium conditions^{3,4}, new experiments revealed resistivity oscillations^{5,6} and zero-resistance states^{7,8}, if a 2D electron gas formed in GaAs/AlGaAs heterostructures is exposed to microwave (MW) radiation. These oscillations are controlled by the ratio of the radiation frequency, ω , to the cyclotron frequency, ω_c . The zero-resistance states (ZRS) are assumed⁹ to be caused by instability of an electron system with absolute negative conductivity, $\sigma_{xx} < 0$, regardless of the actual mechanism of MW-induced resistance oscillations (MIRO) which is still under debate (for a review, see Ref. 10).

Among different theoretical mechanisms proposed for the explanation of MIRO, here we would like to highlight the displacement^{11,12} and inelastic¹³ models. The displacement mechanism is based on a peculiarity of orbit center migration ($X \rightarrow X'$) when an electron absorbs a photon and simultaneously is scattered off impurities. The authors of the inelastic mechanism noticed that photon-assisted scattering affects the distribution function of electrons $f(\varepsilon)$ in such a way that it acquires a nonequilibrium oscillating correction (a sort of population inversion) whose derivative leads to a sign-changing contribution to σ_{xx} .

MW-induced magnetoconductivity oscillations similar to MIRO and even ZRS were observed in a nondegenerate 2D electron gas formed on the free surface of liquid helium^{14,15}. The important distinction of these new oscillations is that they are observed only if the excitation energy of the second surface subband $\Delta_{2,1} \equiv \Delta_2 - \Delta_1$ is tuned to the resonance with the MW field ($\Delta_{2,1} = \hbar\omega$) by varying the pressing electric field (a sort of Stark effect in the 1D potential well formed at the surface). It should be noted also that the shape of these oscillations

strikingly differs from the usual shape of magnetointersubband oscillations described theoretically¹⁶ and observed¹⁷ for semiconductor heterostructures under conditions that two subbands are occupied. Instead of simple peaks of σ_{xx} expected at the conditions of alignment of Landau levels belonging to different subbands, the shape of MIRO observed in a 2D electron gas on liquid helium represents rather a derivative of peaks.

The oscillations reported for electrons on liquid helium were explained¹⁸⁻²⁰ by a nonequilibrium population of the excited subband which triggers quasi-elastic intersubband scattering of electrons with the same peculiarity of orbit center migration as that noticed in the displacement model. Thus, the intersubband mechanism of MIRO and ZRS has something in common with the both displacement and inelastic mechanisms though it does not use the concept of photon-assisted scattering which is important for these two models. Extensive studies of MIRO in a nondegenerate 2D electron gas on liquid helium have revealed a number of remarkable effects associated with the ZRS regime: in-plane redistribution of electrons²¹, self-generated audio-frequency oscillations²², and incompressible states²³. An explanation of these novel observations is based on the concept of electron density domains²⁴: regions of different densities appear to eliminate the regime of negative conductivity.

It should be noted also that even the delicate theoretical predictions reported for the intersubband mechanism of MIRO²⁰ which concern the effect of Coulomb interaction on conductivity extrema were clearly observed in the experiment²⁵. Still, this mechanism of MIRO was described only for a nondegenerate multisubband electron system using an important simplification: $f(\varepsilon) \propto \exp(-\varepsilon/T_e)$, where ε is the in-plane energy, and T_e is the electron temperature. It is not clear how the Pauli exclusion principle affects this mechanism; and the theory does not indicate in what respect the results obtained for electrons on liquid helium can be applied to a degenerate 2D electron system similar to those investigated in semiconductor structures.

In this work we develop a theory of magnetoconductivity oscillations in a degenerate 2D electron gas which are induced by nonequilibrium population of excited subbands. We introduce a new definition of the extended dynamic structure factor of a multisubband 2D electron system which incorporates the concept of quasi-Fermi levels (*imref*) and describes the contribution of elastic intersubband scattering to the momentum relaxation rate under conditions that electron distribution is strongly displaced from equilibrium and cannot be attributed to simple heating of electrons. We demonstrate that nonequilibrium populations of excited subbands can lead to magnetointersubband oscillations whose shape differs from the shape of usual oscillations caused by the equilibrium population of the second subband and the alignment of staircases of Landau levels¹⁶. This induces important changes in quantum magnetotransport of a degenerate 2D electron system and can even lead to negative linear response conductivity.

II. MAGNETOTRANSPORT IN MULTISUBBAND 2D SYSTEMS

Electrons formed on the free surface of liquid helium have a rather low density $n_e \lesssim 2 \times 10^9 \text{ cm}^{-2}$, therefore at temperatures which are comparable with the Fermi temperature they are already localized in sites of the Wigner lattice²⁶. Above the Wigner solid transition temperature this system can be considered as a nondegenerate Coulomb liquid where the Pauli exclusion principle is unimportant. Electrons on a liquid helium film represent a remarkable exception: for a special arrangement of various substrates²⁷ they can form a 2D Fermion system even at $T = 0$.

Electrons in semiconductor structures usually have the effective mass which is much smaller than the free electron mass. Therefore, at low temperatures these electrons can be described as a 2D Fermi gas. A 2D electron system formed in a semiconductor device can have more than one subband^{1,28,29}. There is a number of experiments demonstrated importance of intersubband scattering for electron transport in a 2D system^{17,30}. These results represent properties of an equilibrium system, when the gate potential and the Fermi level position in a GaAs/AlGaAs heterostructure provide the second subband occupancy. There is also a possibility of changing carrier density by illuminating samples with light due to electron-hole pair generation³¹. In this work, we shall focus on magnetotransport properties of a 2D electron system under conditions that electron populations of excited subbands deviate substantially from equilibrium and cannot be described by a single chemical potential.

The energy spectrum of a multisubband 2D electron system in crossed magnetic (B) and electric (E_{\parallel}) fields is described by three quantum numbers (l , n , and X ; here we shall ignore the spin variable):

$$\mathcal{E}_{l,n,X} = \Delta_l + \varepsilon_n + eE_{\parallel}X, \quad (1)$$

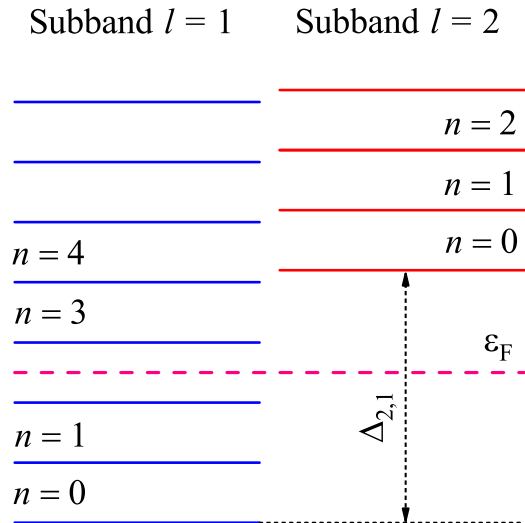


FIG. 1: Schematic illustration of a two-subband 2D electron system in a magnetic field. The energy spectrum of the ground (blue) and the first excited (red) subbands represents a staircase of Landau levels. The position of the Fermi-level at equilibrium is shown by the pink horizontal line.

where Δ_l is the subband energy ($l = 1, 2, \dots$), X is the coordinate of the center of the cyclotron motion, ε_n is the usual Landau spectrum

$$\varepsilon_n = \hbar\omega_c (n + 1/2), \quad (2)$$

($n = 0, 1, \dots$), and $\omega_c = eB/m_e c$ is the cyclotron frequency. In the center-of-mass reference frame moving with regard to the laboratory frame with the drift velocity \mathbf{u}_d , the electric field $E_{\parallel}' \rightarrow 0$ and the in-plane electron motion is described by the pure Landau spectrum of Eq. (2). The degeneracy of each Landau level is given by $S_A/2\pi\ell_B^2$, where $\ell_B = \sqrt{\hbar c/eB}$ is the radius of the cyclotron orbit at $n = 0$, and S_A is the surface area.

The schematic view of Landau levels of a two-subband system is shown in Fig. 1. The Landau levels of the excited subband are up-shifted by $\Delta_{2,1} \equiv \Delta_2 - \Delta_1$ as compared to respective levels of the ground subband. In contrast with the model considered previously¹⁶, the equilibrium Fermi energy ε_F is assumed to be smaller than the intersubband excitation energy $\hbar\omega_{2,1} = \Delta_{2,1}$ (here $\omega_{2,1}$ is the excitation frequency). It is obvious that at certain magnetic fields defined by the condition $\omega_{2,1}/\omega_c = m$ (here $m = 1, 2, \dots$) Landau levels of the excited subband becomes completely aligned with high enough Landau levels of the ground subband which triggers elastic intersubband scattering.

At strong magnetic fields directed perpendicular to the electron layer, magnetotransport of a 2D electron gas is well described³² by the center-migration theory^{33,34}, if the collision broadening of Landau levels is taken into

account. For semiconductor electrons, there are two scattering mechanisms important at low temperatures: Coulomb scattering from charged centers and surface roughness scattering¹. Both of them represent essentially elastic scattering process. Each experimental realization of a 2D electron system has its own specific nature of scatterers. The details of this nature are not important for the effect considering in this work, and they can be incorporated in the theory by changing the matrix elements of electron scattering. As we shall see, the important parameters of the theory are the Landau level broadening and the momentum collision rate at zero magnetic field. Therefore, here we shall model the scatterers by artificial heavy atoms interacting with electrons by an arbitrary potential $V_{\text{int}}(|\mathbf{R}_e - \mathbf{R}_a|)$ (here \mathbf{R}_e and \mathbf{R}_a are radius vectors of an electron and an atom respectively).

In the model considering here, the interaction Hamiltonian can be represented in terms of creation ($a_{\mathbf{K}}^\dagger$) and destruction ($a_{\mathbf{K}}$) operators of atoms as

$$H_{\text{int}} = \frac{1}{\Omega_v} \sum_e \sum_{\mathbf{K}, \mathbf{K}'} \exp[-i(\mathbf{K}' - \mathbf{K}) \cdot \mathbf{R}_e] \times \\ \times V_{|\mathbf{K}' - \mathbf{K}|} a_{\mathbf{K}'}^\dagger a_{\mathbf{K}}, \quad (3)$$

where $\Omega_v \equiv S_A L_z$ is the volume containing these atoms, \mathbf{K} represents a 3D wave vector of an atom, and $V_{|\mathbf{K}' - \mathbf{K}|}$ is a Fourier-transform of the potential $V_{\text{int}}(R)$. For the effective potential $V_a \delta(\mathbf{R}_e - \mathbf{R}_a)$, conventionally describing interaction with short-range scatterers, $V_Q = V_a$. Static defects resulting in elastic electron scattering are described by the limiting case $M_a \rightarrow \infty$ (here M_a is the mass of an artificial atom). Surface defects can be modeled by a 2D layer of artificial atoms. Similar modeling can be considered for a description of remote scatterers.

In the case of a nondegenerate 2D electron gas, the problem of finding the nonequilibrium magnetoconductivity σ_{xx} can be equally well solved by considering the momentum exchange at a collision in the laboratory^{18,20,35} or in the center-of-mass¹⁹ reference frames. For nondegenerate electrons, a great simplification appears because $[1 - f(\varepsilon_{n', X'})] \simeq 1$, and the quantity to be averaged in the laboratory frame is independent of X . This allows one to restrict the averaging procedure to the Landau level index n only, assuming the distribution function $f(\varepsilon_n) \propto \exp(-\varepsilon_n/T_e)$ with an effective temperature T_e .

Magnetoconductivity σ_{xx} of a degenerate 2D electron system can be found from the average friction force \mathbf{F}_{fr} acting on electrons due to interaction with scatterers (the momentum balance method³⁶⁻³⁹) or using a direct expression for the current j_x and calculating probabilities of electron scattering from X to X' (a version of the Titeica's method⁴⁰). In order to avoid complications with the field term $eE_{\parallel}X$ in the energy spectrum of degenerate electrons, it is convenient to consider scattering processes in the center-of-mass reference frame moving with

the drift velocity \mathbf{u}_d with regard to the laboratory reference frame. In this moving frame, the driving electric field E'_{\parallel} is zero³⁹, and the electron spectrum coincides with the Landau spectrum ε_n . It is important that the momentum exchange at a collision $\mathbf{Q} \equiv \mathbf{K}' - \mathbf{K}$ in the center-of-mass frame is the same as in the laboratory frame because of the linear relationship between a momentum and the respective velocity. At the same time, one have to keep in mind that in the center-of-mass reference frame the energy exchange at an elastic collision acquires a Doppler shift correction,³⁹

$$E_{\mathbf{K}'}^{(a)} - E_{\mathbf{K}}^{(a)} = -\hbar \mathbf{Q} \cdot \mathbf{u}_d \equiv -\hbar \mathbf{q} \cdot \mathbf{u}_d, \quad (4)$$

due to the quadratic dependence of the energy of an atom on its velocity. Here $E_{\mathbf{K}}^{(a)} = \hbar^2 K^2 / 2M_a$ and we used the notation $\mathbf{Q} = \{\mathbf{q}, \kappa\}$ with \mathbf{q} and κ standing for the in-plane and vertical components respectively. It is quite obvious that scattering probabilities should not depend on a choice of an inertial reference frame. Physically, the correction of Eq. (4) is equivalent to the energy exchange for the electron spectrum considered in the laboratory frame $eE_{\parallel}(X' - X) = \hbar q_y V_H$, here we have taken into account that $X' - X = q_y \ell_B^2$ due to the momentum conservation and used the notation $V_H = cE_{\parallel}/B$ for the Hall velocity ($u_d^{(y)} \simeq -V_H$).

The momentum balance approach^{38,39} allows obtaining the effective collision frequency of electrons ν_{eff} from the kinetic friction acting on the whole electron system \mathbf{F}_{fr} . In the linear transport regime, \mathbf{F}_{fr} is proportional to \mathbf{u}_d , and conventionally it can be written as⁴¹ $\mathbf{F}_{\text{fr}} = -N_e m_e \nu_{\text{eff}} \mathbf{u}_d$, where the proportionality factor ν_{eff} defines electron magnetoconductivity

$$\sigma_{xx} \simeq \frac{e^2 n_e \nu_{\text{eff}}}{m_e \omega_c^2}, \quad (5)$$

and $n_e = N_e/S_A$ is electron density.

The simplest way of obtaining ν_{eff} is to consider the momentum balance along the y -axis, $F_{\text{fr}}^{(y)} = -N_e m_e \nu_{\text{eff}} u_d^{(y)}$. Assuming $u_d^{(y)} \simeq -V_H$ and using the Born approximation for scattering probabilities in the center-of-mass frame, one can find

$$F_{\text{fr}}^{(y)}(V_H) = -N_e \sum_{\mathbf{q}} \hbar q_y \bar{W}_{\mathbf{q}}(V_H), \quad (6)$$

where

$$\bar{W}_{\mathbf{q}}(V_H) = \frac{2\pi n_a^{(3D)}}{\eta \hbar S_A} \sum_{l, l', n, n'} f_l(\varepsilon_n) [1 - f_{l'}(\varepsilon_{n'})] \times \\ \times J_{n, n'}^2(x_q) U_{l', l}^2(q) \delta(\varepsilon_{n'} - \varepsilon_n + \Delta_{l', l} + \hbar q_y V_H) \quad (7)$$

is the probability of electron scattering with the in-plane momentum exchange equal $\hbar \mathbf{q}$, and $\Delta_{l', l} = \Delta_{l'} - \Delta_l$. Here we have used the following notations: $n_a^{(3D)}$ is the

density of scatterers, $\eta = 2\pi\ell_B^2 n_e$ is the filling factor, $f_l(\varepsilon_n)$ is the electron distribution function, the functions $U_{l',l}^2(q)$ and $I_{n,n'}^2(x_q)$ are defined by matrix elements of the interaction Hamiltonian

$$U_{l',l}^2(q) = \frac{1}{L_z} \sum_{\kappa} V^2 \sqrt{q^2 + \kappa^2} \left| (e^{-i\kappa z})_{l',l} \right|^2, \quad (8)$$

$$\left| (e^{-i\mathbf{q}\cdot\mathbf{r}_e})_{n',X';n,X} \right|^2 = \delta_{X,X' - \ell_B^2 q_y} I_{n,n'}^2(x_q), \quad (9)$$

$$I_{n,n'}^2(x) = \frac{[\min(n,n')!]}{[\max(n,n')!]} x^{|n-n'|} e^{-x} \left[L_{\min(n,n')}^{|n-n'|}(x) \right]^2,$$

$x_q = q^2 \ell_B^2 / 2$, and $L_n^m(x)$ are the associated Laguerre polynomials. When obtaining Eq. (7), we used the advantages of describing scattering probabilities in the moving frame - the summations over indexes X , X' and \mathbf{K} are trivial leading to the factors $n_B = 1/2\pi\ell_B^2$ and $n_a^{(3D)}$.

Comparing the right side of Eq. (6) with the result expected for the linear regime $N_e m_e \nu_{\text{eff}} V_H$, one can find that

$$\nu_{\text{eff}} = -\frac{1}{m_e V_H} \sum_{\mathbf{q}} \hbar q_y \bar{W}_{\mathbf{q}}(V_H). \quad (10)$$

When expanding $\bar{W}_{\mathbf{q}}(V_H)$ in V_H , we can consider only the linear term $\bar{W}'_{\mathbf{q}}(0) V_H$ [here the 'prime' denotes the differentiation] because $\bar{W}_{\mathbf{q}}(0)$ depends only on the absolute value of \mathbf{q} and, therefore, gives zero contribution into ν_{eff} .

It is instructive to note that the same result for ν_{eff} and σ_{xx} can be found from the direct expression for the electron current along x -direction (this method was also used^{42,43} for describing a nondegenerate electron system):

$$j_x = -en_e \sum_{\mathbf{q}} (X' - X)_{\mathbf{q}} \bar{W}_{\mathbf{q}}(V_H), \quad (11)$$

where we have to use the relationship $(X' - X)_{\mathbf{q}} = \ell_B^2 q_y$ which follows from matrix elements of Eq. (9). The Eq. (11) and the definition of σ_{xx} obviously yield the expression for ν_{eff} given in Eq. (10).

To obtain a finite magnetoconductivity in the treatment presented above, one have to include higher approximations by incorporating the collision broadening of Landau levels $\Gamma_{l,n}$ (the broadening of electron density of states). Following the ideas of the center migration theory³³ and the self-consistent Born approximation (SCBA)³², in the right side of Eq. (7) we shall insert $\int d\varepsilon \int d\varepsilon' \delta_l(\varepsilon - \varepsilon_n) \delta_{l'}(\varepsilon' - \varepsilon_{n'})$; the subscripts l and l' in the respective delta-functions just mark the subband where the level density belongs. Then, assuming the replacement $\delta_l(\varepsilon - \varepsilon_n) \rightarrow -\frac{1}{\pi\hbar} \text{Im}G_{l,n}(\varepsilon)$ [here $G_{l,n}(\varepsilon)$ is the single-electron Green's function], the average probability of scattering with the momentum exchange $\hbar\mathbf{q}$ can

be represented in the following form:

$$\bar{W}_{\mathbf{q}}(V_H) = \frac{n_a^{(3D)}}{S_A \hbar^2} \sum_{l,l'} U_{l',l}^2(q) D_{l,l'}(q, \omega_{l,l'} - q_y V_H), \quad (12)$$

where $\omega_{l,l'} = \Delta_{l,l'}/\hbar$, and

$$D_{l,l'}(q, \Omega) = \frac{2}{\pi\hbar\eta} \int d\varepsilon f_l(\varepsilon) [1 - f_{l'}(\varepsilon + \hbar\Omega)] \times \\ \times \sum_{n,n'} I_{n,n'}^2(x_q) \text{Im}G_{l,n}(\varepsilon) \text{Im}G_{l',n'}(\varepsilon + \hbar\Omega) \quad (13)$$

is a new generalization of the dynamic structure factor (DSF) of a multisubband 2D electron system. Expanding $\bar{W}_{\mathbf{q}}$ in $q_y V_H$ yields

$$\nu_{\text{eff}} = \frac{n_a^{(3D)}}{m_e \hbar S_A} \sum_{\mathbf{q}} \sum_{l,l'} q_y^2 U_{l',l}^2(q) D'_{l,l'}(q, \omega_{l,l'}) . \quad (14)$$

Thus, the effective collision frequency of a multisubband 2D electron system is proportional to the derivative of the extended DSF $D'_{l,l'}(q, \omega_{l,l'})$ with respect to frequency.

There are two important approximations for the Landau level density of states. The SCBA theory of Ando and Uemura yields the semi-elliptical shape of the density of states³²

$$-\text{Im}G_n(\varepsilon) = \frac{2\hbar}{\Gamma_n} \sqrt{1 - \frac{(\varepsilon - \varepsilon_n)^2}{\Gamma_n^2}}, \quad (15)$$

where Γ_n is the broadening parameter. In the case of short-range scatterers, Γ_n is independent of Landau number $\Gamma_n = \Gamma$ with³²

$$\Gamma = \sqrt{\frac{2}{\pi} \hbar \omega_c \nu_0}, \quad (16)$$

where ν_0 is the electron relaxation rate obtained for $B = 0$. The cumulant expansion method⁴⁴ yields the Gaussian shape of Landau levels

$$-\text{Im}G_n(\varepsilon) = \frac{\sqrt{2\pi}\hbar}{\Gamma_n} \exp\left[-\frac{2(\varepsilon - \varepsilon_n)^2}{\Gamma_n^2}\right], \quad (17)$$

which does not have the sharp cutoff of the density of states. Generally, the level shape is a kind of mixture of elliptical and Gaussian forms⁴⁵, and the shape of the lowest level is close to a Gaussian.

In the case of equilibrium Fermi-distribution, $D_{l,l'}(q, \Omega)$ has very useful properties which simplify significantly evaluation of ν_{eff} and σ_{xx} . For example, consider only the contribution from intrasubband scattering processes ($l' = l$). Then, $D_{l,l}(q, \Omega)$ coincides with the conventional DSF of a 2D electron system which satisfies the condition

$$D_{l,l}(q, -\Omega) = e^{-\hbar\Omega/T_e} D_{l,l}(q, \Omega) \quad (18)$$

The derivative of this relationship gives $D'_{l,l}(q, 0) = \frac{\hbar}{2T_e} D_{l,l}(q, 0)$ and the linear (in $q_y V_H$) term of Eq. (12) can be rewritten as

$$\delta \bar{W}_{\mathbf{q}} \simeq -q_y V_H \frac{\hbar}{2T_e} \bar{W}_{\mathbf{q}}(0), \quad (19)$$

which allows representing σ_{xx} in terms of the equilibrium probability $\bar{W}_{\mathbf{q}}(0)$:

$$\sigma_{xx} \simeq \frac{e^2 n_e}{2T_e} \sum_{\mathbf{q}} (X' - X)_{\mathbf{q}}^2 \bar{W}_{\mathbf{q}}(0). \quad (20)$$

This equation coincides with the well-known result obtained previously^{33,46}, and it is similar to the Einstein relation between the conductivity and the diffusion coefficient.

For the ground subband and the semi-elliptic shape of Landau levels [Eq. (15)] induced by short-range scatterers, Eq. (20) transforms into the result of Ando and Uemura which indicates that the conductivity peak value $(\sigma_{xx})_{\max} = \frac{e^2}{\pi^2 \hbar} (n + 1/2)$ depends only on the Landau level index n and the natural constants³². These "check-points" of equilibrium transport regime, encourage us to use Eq. (14) for describing magnetotransport in nonequilibrium multisubband 2D electron systems.

For a nonequilibrium filling of 2D subbands, the extended DSF $D_{l,l'}(q, \Omega)$ generally has no a relationship similar to Eq. (18). Only describing nondegenerate electrons and assuming $f_l(\varepsilon) \propto N_l \exp(-\varepsilon/T_e)$ it was possible to introduce^{19,20} a version of the DSF $S_{l,l'}(q, \Omega)$ which had an important property resembling Eq. (18), in spite of the fact that the occupation of subbands was not equilibrium. Unfortunately, this version of the extended DSF appears to be useless for degenerate electrons. The new definition of the extended DSF $D_{l,l'}(q, \Omega)$ given in Eq. (13) transforms into $\bar{n}_l S_{l,l'}(q, \Omega)$ if the electron system can be considered as a nondegenerate gas [here $\bar{n}_l = N_l/N_e$ is the fractional occupancy of a subband].

III. QUASI-FERMI LEVEL APPROXIMATION

Generally, it is very difficult to find $f_l(\varepsilon)$ if a system is displaced from equilibrium. Therefore, in solid state physics it is quite common to use the concept of a quasi-Fermi level or *imref*. In the following, we assume that displacement from equilibrium is such that electron populations can no longer be described by a single chemical potential (or a Fermi level), nevertheless it is possible to describe it introducing separate chemical potentials (quasi-Fermi levels) for each subband:

$$f_l(\varepsilon) = \frac{1}{e^{(\varepsilon + \Delta_{l,1} - \mu_l)/T_e} + 1} \equiv f_F(\varepsilon + \Delta_{l,1} - \delta\mu_l), \quad (21)$$

where $\delta\mu_l = \mu_l - \mu$. The chemical potentials μ_l are measured from the bottom of the ground subband, while the zero of Landau energy ε is taken at the bottom of each

subband. In most cases, it is sufficient to consider only two subbands (the ground subband and the first excited subband), when electron populations of higher subbands can be neglected. The form of Eq. (21) is quite accurate if electron-electron collisions are more important for intrasubband redistribution than for intersubband decay rates. Anyway, this form of $f_l(\varepsilon)$ is very useful because it allows obtaining σ_{xx} in an analytical form for nonequilibrium populations of electron subbands.

One can also introduce different electron temperatures for each subband ($T_{l,e}$), still we shall assume that $T_{l,e} = T_{l',e} = T_e$ because in-plane energy relaxation between different subbands is governed by electron-electron collisions (electron spacing is usually much larger than the average distance between nearest subbands), whose rate is quite high for 2D electron systems¹. Regarding possible heating of electrons ($T_e > T$), we assume that T_e is still much lower than the quasi-Fermi energies. The opposite limiting case (nondegenerate electrons) was described in Refs. 19,20. It should be noted also that MIRO observed in a 2D electron gas on liquid helium are quite well described even by the approximation $T_e = T$ in spite of a substantial heating²⁵.

Using the distribution function of Eq. (21) and the well-known identity

$$f_F(\varepsilon) [1 - f_F(\varepsilon')] = [f_F(\varepsilon) - f_F(\varepsilon')] \frac{1}{1 - e^{(\varepsilon - \varepsilon')/T_e}}, \quad (22)$$

it is possible to establish the following relationship for the extended DSF⁴⁷

$$D_{l',l}(q, -\Omega) = e^{-(\hbar\Omega + \Delta_{l',l} - \mu_{l',l})/T_e} D_{l,l'}(q, \Omega), \quad (23)$$

where $\mu_{l',l} = \mu_{l'} - \mu_l$. For a single subband ($l' = l$), this property coincides with the property of the usual DSF of a 2D electron gas given in Eq. (18).

When considering the contribution from intersubband scattering ν_{inter} in Eq. (14), the property of Eq. (23) allows us to transform derivatives of the DSF whose frequency argument is negative into functions with a positive argument

$$D'_{l',l}(q, -\Omega) = -e^{-(\hbar\Omega + \Delta_{l',l} - \mu_{l',l})/T_e} D'_{l,l'}(q, \Omega) + \frac{\hbar}{T_e} e^{-(\hbar\Omega + \Delta_{l',l} - \mu_{l',l})/T_e} D_{l,l'}(q, \Omega) \quad (24)$$

Thus, a substantial part of $D'_{l,l'}(q, \omega_{l,l'})$ entering Eq. (14) can be eliminated by reverse scattering processes due to the first term in the right side of Eq. (24). Therefore, it is convenient to represent the contribution of intersubband scattering to ν_{eff} in the form containing only positive frequency arguments ($l > l'$). In this way, one can obtain two kinds of contributions: a normal contribution proportional to $D_{l,l'}(q, \omega_{l,l'})$, and an abnormal (sign-changing) contribution proportional to the derivative $D'_{l,l'}(q, \omega_{l,l'})$. To make a distinction between

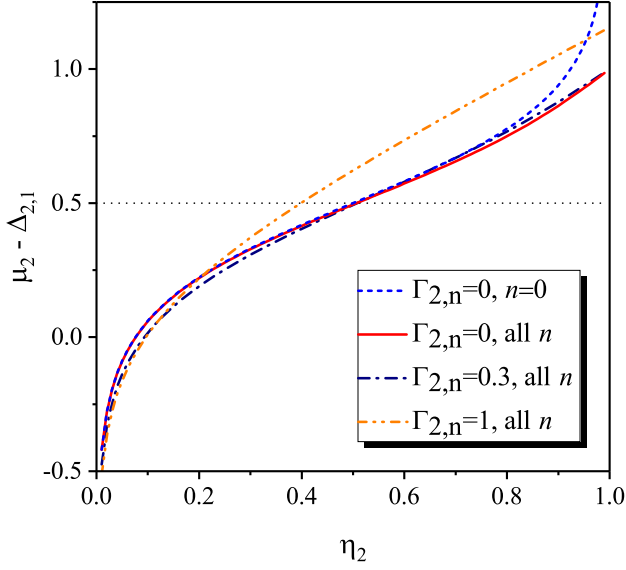


FIG. 2: The quasi-chemical potential of the first excited subband $\mu_2 - \Delta_{2,1}$ (in units of $\hbar\omega_c$) versus the filling factor $\eta_2 = 2\pi\ell_B^2 N_2/S_A$ calculated for different conditions which are indicated in the figure legend. The level broadening $\Gamma_{2,n}$ is also shown in units of $\hbar\omega_c$.

these contributions, we shall use the following notations: $\nu_{\text{inter}} = \nu_N + \nu_A$, where

$$\nu_N = \frac{n_a^{(3D)}}{m_e \hbar S_A} \sum_{l>l'} \sum_{\mathbf{q}} \frac{\hbar}{T_e} q_y^2 U_{l',l}^2(\mathbf{q}) e^{-\mu_{l,l'}/T_e} D_{l,l'}(q, \omega_{l,l'}), \quad (25)$$

$$\begin{aligned} \nu_A &= \frac{n_a^{(3D)}}{m_e \hbar S_A} \sum_{l>l'} \left(1 - e^{-\mu_{l,l'}/T_e}\right) \times \\ &\times \sum_{\mathbf{q}} q_y^2 U_{l',l}^2(\mathbf{q}) D'_{l,l'}(q, \omega_{l,l'}). \end{aligned} \quad (26)$$

The normal contribution ν_N exists even under the equilibrium condition ($\mu_{l,l'} = 0$), though at $\mu < \Delta_{l,l'}$ it is very small due to $f_l(\varepsilon)$ present in $D_{l,l'}(q, \omega_{l,l'})$. The abnormal terms ν_A differ from zero only if electron distribution is somehow displaced from equilibrium ($\mu_{l,l'} > 0$).

When the first excited subband ($l = 2$) has an extra electron population δN_2 , one expects that the all these electrons will occupy the lowest Landau level ($n = 0$), if low temperatures ($T_e \ll \hbar\omega_c$) are considered and the filling factor of the excited subband $\eta_2 = 2\pi\ell_B^2 N_2/S_A < 1$. Neglecting electron populations at higher Landau levels and assuming that the level broadening is small, one can find the quasi-Fermi level of the excited subband

$$\mu_2 = \Delta_{2,1} + \varepsilon_0 - T_e \ln \left(\frac{1 - \eta_2}{\eta_2} \right). \quad (27)$$

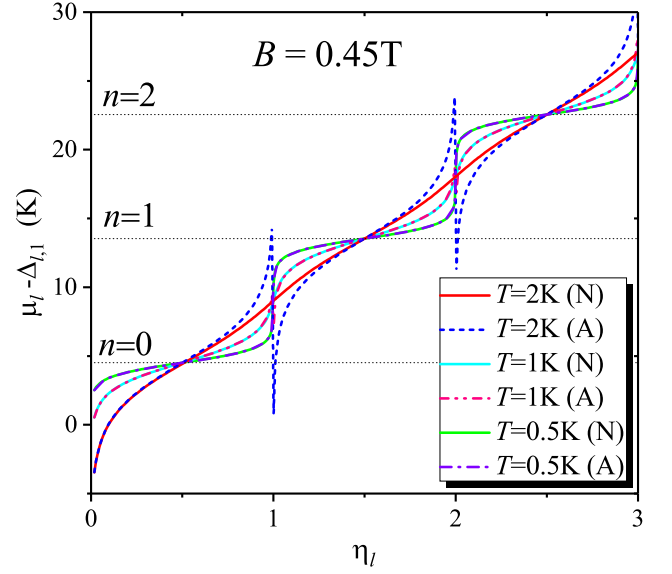


FIG. 3: The analytical (A) extension of the quasi-chemical potential of the l -subband (dashed, dash-dotted and dash-dot-dotted lines) is compared with the results of numerical (N) calculations for narrow Landau levels (solid lines). The wavy shape of the solid lines increases with lowering temperature together with the accuracy of the analytical approximation.

In this equations, the last two terms represent the well-known high-field approximation for the chemical potential⁴⁸.

The influence of higher Landau levels and a finite broadening $\Gamma_{2,0}$ on $\mu_2(\eta_2)$ is illustrated in Fig. 2 for $\hbar\omega_c/T_e = 5$ (in this figure $\mu_2 - \Delta_{2,1}$ and $\Gamma_{2,n}$ are given in units of $\hbar\omega_c$). These results indicate that the simple form of Eq. (27) describes the dependence $\mu_2(\eta_2) - \Delta_{2,1}$ quite well if $\Gamma_{2,0}/\hbar\omega_c \leq 0.3$. At $\Gamma_{2,0}/\hbar\omega_c = 0.1$, it is even difficult to see the difference between results of numerical calculations (not shown in Fig. 2) and the approximation $\Gamma_{2,0} = 0$ illustrated in the figure by the red line. For the strong broadening $\Gamma_{2,0}/\hbar\omega_c = 1$, the results of numerical calculations (orange line) deviate substantially from the approximation given in Eq. (27), if $\eta_2 > 0.2$. Under these conditions, the analytical form can be used only for a qualitative analysis or simple estimations. It is important that considering a 2D electron system with narrow Landau levels, the approximation of Eq. (27) can be used even for substantial values of the filling factor $\eta_2 \leq 0.8$ which are quite sufficient for this research. The accuracy of the high field approximation increases with lowering temperature.

For larger values of the filling factor $\eta_2 > 1$, one can find a simple extension of the analytical form of Eq. (27) which can be used for the ground subband as well. Therefore, in the following equation, we shall use an arbitrary

subband index (l):

$$\mu_l - \Delta_{l,1} = \sum_{n=0}^{\infty} \left[\varepsilon_n - T_e \ln \left(\frac{n+1-\eta_l}{\eta_l-n} \right) \right] \times \\ \times \theta(n+1-\eta_l) \theta(\eta_l-n), \quad (28)$$

where $\theta(x)$ is the Heaviside step function, and $\eta_l = 2\pi\ell_B^2 N_l / S_A$. This solution is found assuming that $f_l(\varepsilon) \simeq 1$ for $\varepsilon \leq \varepsilon_{n-1}$ if $n < \eta_l < n+1$, therefore it is a low temperature approximation. Fig. 3 illustrates that at low temperatures ($T_e \leq 1$ K) numerical results shown by solid lines, are well approximated by the periodic extension of the high field formula of Eq. (27) given in Eq. (28). Deviations of Eq. (28) from the numerical result appear only in very narrow regions near the points $\eta_l = 1, 2, \dots$. At high temperatures $T_e \gtrsim 0.2 \hbar\omega_c$, the deviations are strong because the numerical results shown by the red line approach the semi-classical formula $\mu_l(\eta_l) - \Delta_{l,1} \simeq 2\pi\hbar^2 N_l / m_e S_A$. In our numerical calculations (here and below), the ratio of the effective electron mass to the free electron mass is fixed to the value 0.067 which is typical for semiconductor heterostructures.

In Fig. 3, the filling factor η_l was varied by changing electron density $n_l = N_l / S_A$, while the magnetic field was fixed. It is remarkable that the simple analytical approximation given in Eq. (28) can be used also for the description of the well-known oscillations⁴⁹ of the chemical potential $\mu(B)$ of a 2D electron system with a fixed density and narrow Landau levels (here we omit the subband index). This possibility is illustrated in Fig. 4 for $n_e = 1.5 \times 10^{10} \text{ cm}^{-2}$ and $T = 0.5$ K, assuming that the broadening of Landau levels is small. One can see that the analytical formula (red line) practically coincides with the results of numerical calculations (blue line) in a wide range of magnetic fields with the exception of the points where $\eta(B)$ is very close to an integer (1, 2, ...) as indicated in Fig. 4.

IV. RESULTS AND DISCUSSION

According to Eqs. (25) and (26) the contribution from intersubband scattering to the effective collision frequency as a function of the magnetic field is determined by the extended DSF $D_{l,\nu}(q, \Omega)$ and its derivative with respect to frequency $D'_{l,\nu}(q, \Omega)$ near the special points $\Omega = \omega_{l,\nu} \equiv \Delta_{l,\nu} / \hbar > 0$. Considering the two subband model ($l = 2$ and $l' = 1$), in Eq. (13) which defines $D_{2,1}(q, \Omega)$ the factor $[1 - f_1(\varepsilon + \hbar\Omega)]$ can be set to unity because the distribution function of electrons occupying the ground subband is very small at high energies: $f_1(\varepsilon + \Delta_{2,1}) \ll 1$. The later inequality follows from the fact that the respective quasi Fermi level $\mu_1 \leq \mu$. For the regime of fixed density, $\mu_1 < \mu$ which is quite obvious according to Fig. 3. In the the regime of fixed chemical potential, $\mu_1 = \mu$ due to a reservoir of electrons⁴⁸. Therefore, the nonequilibrium DSF $D_{2,1}(q, \Omega)$

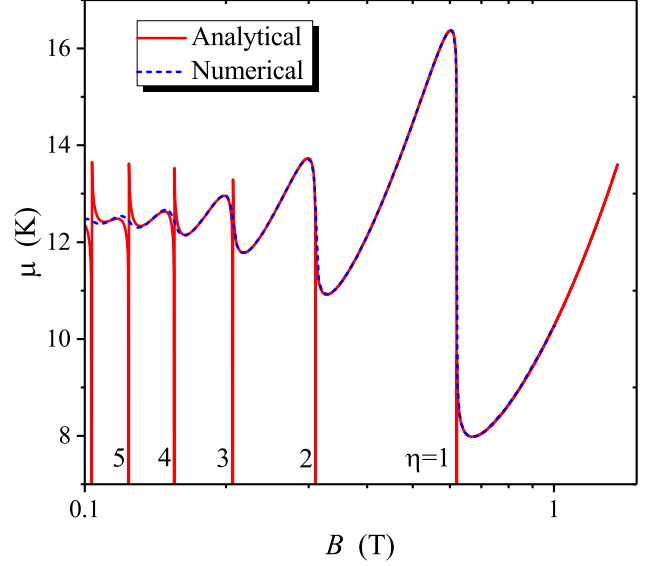


FIG. 4: Illustration of the efficiency of the analytical approximation given in Eq. (28) for the description of oscillations of the chemical potential (Fermi energy) as a function of B under conditions that the collision broadening is small: the analytical equation (solid red line), and numerical calculations (dashed blue line). The singular points, where the filling factor η equals to an integer, are indicated.

as a function of frequency is determined mostly by the distribution of electrons occupying the excited subband

$$f_2(\varepsilon) = \left\{ \frac{1-\eta_2}{\eta_2} \exp\left(\frac{\varepsilon-\varepsilon_0}{T_e}\right) + 1 \right\}^{-1}, \quad (29)$$

where we had used the approximation of Eq. (27) for μ_2 assuming that $\eta_2 \leq 0.8$. For larger η_2 , we shall use the extension of Eq. (28).

In the expression for the effective collision frequency ν_{eff} , the DSF is affected by integration over q . For short-range scatterers, the respective integral can be easily calculated because $\int x_q I_{n,n'}^2(x_q) dx_q = (n+n'+1)$. Therefore, it is convenient to analyze the frequency dependence of the dimensionless function

$$J_{2,1}(\omega/\omega_c) = \frac{\eta\Gamma}{4\hbar} \int_0^{\infty} D_{2,1}(q, \omega) x_q dx_q \quad (30)$$

instead of $D_{2,1}(q, \omega)$. Here, for simplicity reasons, the collision broadening of Landau levels Γ is assumed to be independent of quantum numbers n and l . Employing the Gaussian shape of $\text{Im}G_{l,n}(\varepsilon)$ given in Eq. (17) yields

$$J_{2,1} = \eta_2 \sum_{n=1}^{\infty} (n+1) \int_{-\varepsilon_0/\Gamma}^{\infty} \frac{\exp(-2y^2)}{(1-\eta_2) \exp(y\Gamma/T_e) + \eta_2} \times \\ \times \exp\left\{ -2 \left[y + \frac{\hbar\omega_c}{\Gamma} \left(\frac{\omega}{\omega_c} - n \right) \right]^2 \right\} dy. \quad (31)$$

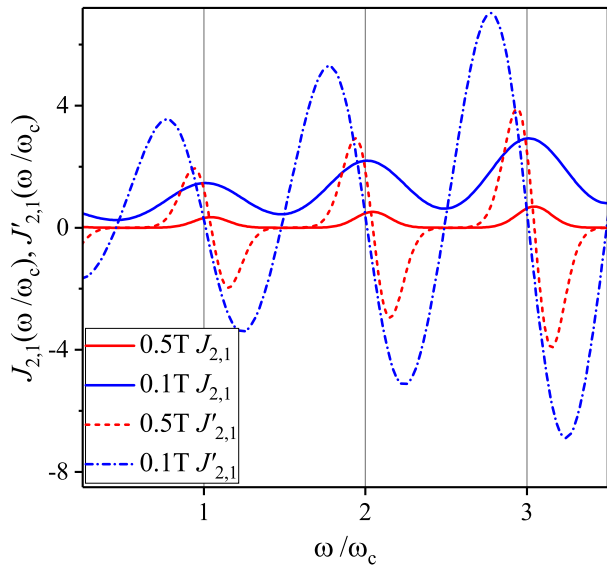


FIG. 5: The frequency dependencies of the dimensionless functions which define the shape of magnetooscillations of ν_N and ν_A calculated for two values of the magnetic field shown in the figure legend: $J_{2,1}(\omega/\omega_c)$ (solid lines) and $J'_{2,1}(\omega/\omega_c)$ (dashed and dash-dotted lines).

It is obvious that $J_{2,1}(\omega/\omega_c)$ has prominent maxima near the conditions $\omega/\omega_c = 1, 2, \dots$, if the 2D electron system is pure enough and $\hbar\omega_c/\Gamma > 1$. The results of numerical evaluations of the function $J_{2,1}(\omega/\omega_c)$ and its derivative $J'_{2,1}(\omega/\omega_c)$ are shown in Fig. 5 by the solid and dashed (dashed-dotted) lines respectively. The calculations were performed for $N_2 = 0.1N_e$ and two values of the magnetic field [$B = 0.5$ T (red lines) and 0.1 T (blue lines)]. The heights of the maxima increase with lowering B due to the factor $(1 - \eta_2)/\eta_2$ because the filling factor η_2 (0.5 T) $\simeq 0.165$ while η_2 (0.1 T) $\simeq 0.827$. The change of B affects notably also the positions of minima, maxima and the zero-crossing (sign-changing) point of the derivative $J'_{2,1}(\omega/\omega_c)$.

Using the same approximations as those used for obtaining Eq. (31), the abnormal contribution to the effective collision frequency can be represented as

$$\nu_A = \nu_0 \frac{2p_{2,1}}{\pi\eta} \left(\frac{\hbar\omega_c}{\Gamma} \right)^2 \left(1 - e^{-\mu_{2,1}/T_e} \right) \Phi_{2,1}(B), \quad (32)$$

where we defined

$$\Phi_{2,1}(B) = \frac{\Gamma}{\hbar\omega_c} J'_{2,1}(\omega_{2,1}/\omega_c) \quad (33)$$

because the derivative $J'_{2,1}(\omega_{2,1}/\omega_c)$ contains the additional factor $\hbar\omega_c/\Gamma$ according to Eq. (31). The dimensionless parameter $p_{l,\nu}$ is determined by the following matrix elements

$$p_{l,\nu} = \frac{B_{1,1}}{B_{l,\nu}}, \quad B_{l,\nu}^{-1} = L_z^{-1} \sum_{\kappa} \left| (e^{-i\kappa z})_{\nu,l} \right|^2. \quad (34)$$

The accurate calculation of $p_{2,1}$ requires the knowledge of the details of a particular 2D electron system such as the wavefunctions of subband states which are not considering in this work. For electrons on liquid helium⁵⁰, $p_{2,1}$ is a factor of two smaller than $p_{1,1} = 1$. Therefore, in following numerical calculations we shall use a rough estimation: $2p_{2,1} \simeq 1$.

Under the conditions used for obtaining Eq. (32), the contribution from electron scattering within the ground subband ($l = 1$) can be found as

$$\nu_{\text{intra}}^{(1)} \simeq \nu_0 \frac{p_{1,1}}{\pi\eta} \left(\frac{\hbar\omega_c}{\Gamma} \right)^2 \Phi_{1,1}(B), \quad (35)$$

where

$$\Phi_{1,1}(B) = \sum_{n=0}^{\infty} (2n+1) \exp \left[-\frac{4(\mu_1 - \varepsilon_n)^2}{\Gamma^2} \right]. \quad (36)$$

At the same time, the contribution from electron scattering within the first excited subband $\nu_{\text{intra}}^{(2)}$ has a very weak dependence on B because the distribution function $f_2(\varepsilon)$ given in Eq. (29) varies strongly near ε_0 . Thus, $\nu_{\text{intra}}^{(2)}$ can be considered as a small background value when the ratio $N_2/N_e \ll 1$. The background value decreases also with narrowing of the density of states. In the following, we shall neglect $\nu_{\text{intra}}^{(2)}$ and assume that $\nu_{\text{intra}} \simeq \nu_{\text{intra}}^{(1)}$.

Comparing ν_A of Eq. (32) with $\nu_{\text{intra}}^{(1)}$ given in Eq. (35) indicates that the abnormal contribution contains the additional factor $(1 - e^{-\mu_{2,1}/T_e})$ which is zero under equilibrium conditions ($\mu_2 = \mu_1 = \mu_F$). If we have a nonequilibrium population of the second subband, then, according to Eq. (27) and Fig. 2, $\delta\mu_2$ becomes substantially larger than T_e already at a small filling factor η_2 . For example, Fig. 2 shows that $\mu_2 > \Delta_{2,1}$ if $\eta_2 > 0.1$. Assuming this reasonable condition, we can neglect the exponentially small term in the factor $(1 - e^{-\mu_{2,1}/T_e})$ and set this factor to unity even if μ_1 is fixed (according to Fig. 3, μ_1 decreases with lowering N_1 which also reduces $e^{-\mu_{2,1}/T_e}$).

Another important distinction between ν_A and ν_{intra} is caused by different behaviors of the dimensionless functions $\Phi_{2,1}(B)$ and $\Phi_{1,1}(B)$ illustrated in Fig. 6. The both functions oscillate with varying $1/B$, but the periods of these oscillations are different. Assuming μ_1 is fixed to μ_F , the maxima of the positive function $\Phi_{1,1}(B)$ entering ν_{intra} occur at $\hbar\omega_c = \mu_F/(n+1/2)$ due to the Shubnikov-de Haas effect. In contrast to $\Phi_{1,1}(B)$, the function $\Phi_{2,1}(B)$, which determines ν_A , is a sign-changing function having maxima and minima, according to the definition of Eq. (33) and Fig. 5; its zero-crossing points occur at magnetic fields which are close to the condition $\Delta_{2,1}/\hbar\omega_c = m$ (here $m = 1, 2, \dots$).

It is instructive to analyze ν_N using the same approximations and conditions. Direct transformation of Eq. (25) yields

$$\nu_N = \nu_0 \frac{2p_{2,1}}{\pi\eta} e^{-\mu_{2,1}/T_e} \frac{\hbar^2\omega_c^2}{T_e\Gamma} J_{2,1}(\omega_{2,1}/\omega_c). \quad (37)$$

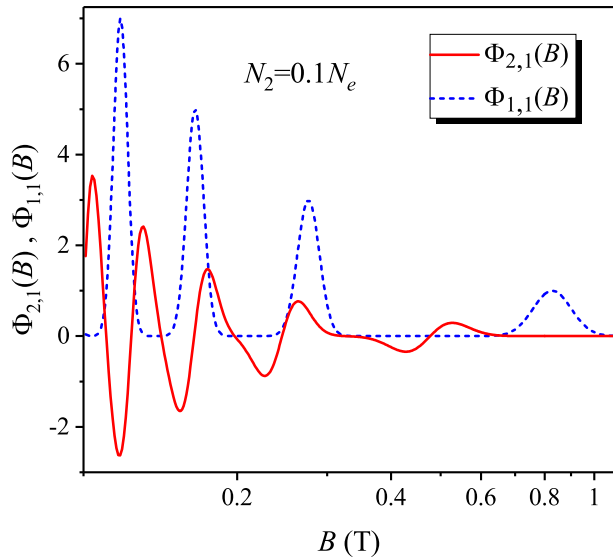


FIG. 6: Graphical illustration of the functions $\Phi_{2,1}(B)$ and $\Phi_{1,1}(B)$ which determine ν_A and ν_{intra} respectively.

As compared to the contribution from intrasubband scattering of Eq. (35), here we have T_e in the denominator because for intersubband scattering one cannot use the relationship $f(\varepsilon)[1-f(\varepsilon)] \rightarrow T_e\delta(\varepsilon - \varepsilon_F)$. The shape of oscillations caused by ν_N is determined by the function $J_{2,1}(\omega_{2,1}/\omega_c)$ shown above in Fig. 5 by solid lines. This shape is in a qualitative accordance with results obtained for magnetointersubband oscillations under equilibrium conditions¹⁶. For nonequilibrium regime described here, Eq. (37) contains also the exponential factor $\exp(-\mu_{2,1}/T_e)$ which becomes very small even for relatively weak excitations $N_2 = 0.1N_e$. It should be noted also that under conditions used here, the amplitude of $\Phi_{2,1}$ is about 5 times larger than the respective amplitude of $J_{2,1}$. Therefore, ν_N can be neglected as compared to ν_A and ν_{intra} .

Typical dependencies of $\sigma_{xx}(B)$ are shown in Fig. 7. In the equilibrium case ($\mu_1 = \mu_2$), $\nu_{\text{eff}} = \nu_{\text{intra}}$ and $\sigma_{xx}(B)$ has maxima when $\hbar\omega_c = \mu_F/(n+1/2)$ according to the SCBA theory³² (blue dashed line). In this figure, the electron conductivity σ_{xx} is normalized by the first ($n=0$) peak value $\sigma_{\text{max}}^{(0)} = e^2/4\pi\hbar$ found for the Gaussian level density ($B \simeq 0.827$ T). Already a small nonequilibrium electron population of the excited subband ($N_2/N_e = 0.1$) induces important changes into $\sigma_{xx}(B)$ shown in Fig. 7 by the red line. Besides additional maxima and a substantial reduction of the SCBA peak at $n=3$, there are sign-changing variations of $\sigma_{xx}(B)$ near $B \simeq 0.48$ T, 0.24 T and 0.156 T, and quite deep minima with regions where the linear response conductivity σ_{xx} becomes negative. An increase in the electron population of the excited subband ($N_2/N_e = 0.2$) amplifies these unusual phenomena as indicated in Fig. 7

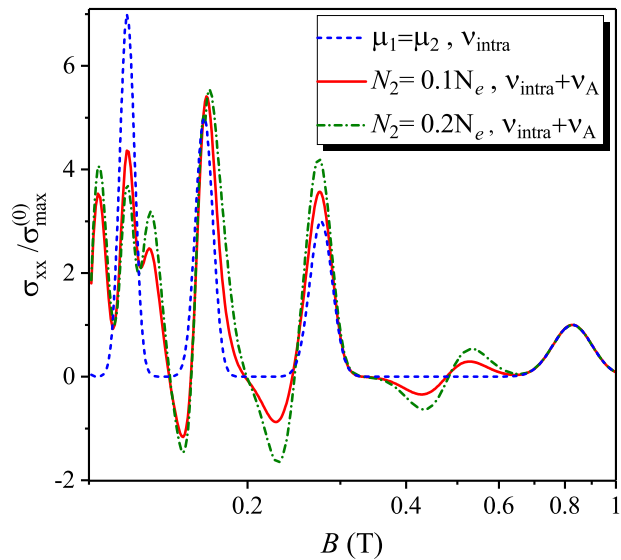


FIG. 7: Magnetoconductivity normalized to $\sigma_{\text{max}}^{(0)} = e^2/4\pi\hbar$ versus the magnetic field for different levels of the displacement from equilibrium: $N_2 \simeq 0$ (blue dashed line), $N_2 = 0.1N_e$ (red solid line), and $N_2 = 0.2N_e$ (olive dash-dotted line).

by the olive dash-dotted line. It should be noted that for such a population, $\eta_2(B)$ becomes larger than unity in the region of low B , and, therefore, the approximation of Eq. (27) defining μ_2 fails. In this case, we had used the extension of the quasi-Fermi energy given in Eq. (28). Numerical calculations indicate also that reducing temperature from 1 K to 0.5 K amplifies additionally the effect of the sign-changing contribution ν_A .

Thus, the theoretical analysis given above indicates that the Pauli exclusion principle does not ruin the intersubband mechanism of MIRO, if the electron distribution in the ground and excited subbands can be described by the quasi-Fermi level approximation. Moreover, a sharp increase of the imref of the excited subband as a function of the filling factor shown in Fig. 2 reduces strongly the compensational contribution from reverse intersubband scattering [the exponential term in parenthesis of Eq. (32); under conditions of Fig. 7 this term does not exceed 0.04]. This means that magnetoconductivity oscillations and ZRS induced by the resonant MW field, whose polarization direction is perpendicular to the electron layer, can be realized in sufficiently clean semiconductor devices. The regions with negative linear response conductivity attract a special interest, because they allow performing complementary studies of ZRS in heterostructures caused by a definite mechanism. These studies potentially can help also with the identification of the origin of MIRO and ZRS in the conventional setup.

V. CONCLUSION

We have presented a theory of quantum magnetotransport in a degenerate multisubband electron system under conditions that electron distributions over 2D subbands cannot be described by a single chemical potential. Using the concept of quasi-Fermi levels and the self-consistent Born approximation, we expressed magnetoconductivity equations in terms of the extended dynamic structure factor and its derivative with regard to frequency. We have shown that a displacement from the equilibrium electron distribution over excited subbands, which cannot be re-

duced to trivial heating, leads to appearance of abnormal sign-changing contribution to the momentum collision rate and magnetoconductivity. Calculations performed for a simplified potential of scatterers indicate that even a small fraction of electrons (about 10%) transferred to the first excited subband can drastically change the shape of magnetointersubband oscillations and lead to negative linear response conductivity. The theory can be applied to electrons on helium films with a special arrangement of substrates²⁷, and to multisubband 2D electron systems of semiconductor devices.

-
- * E-mail: monarkha@ilt.kharkov.ua
- ¹ T. Ando, A.B. Fowler, and F. Stern, *Rev. Mod. Phys.* **54**, 437 (1982).
 - ² *Quantum Hall Effect*, edited by R.E. Prange and S.M. Girvin, (Springer-Verlag, Berlin 1987).
 - ³ von K. Klitzing, G. Dorda, and M. Pepper, *Phys. Rev. Lett.* **45**, 494 (1980).
 - ⁴ D.C. Tsui, H.L. Stormer, and A.C. Gossard, *Phys. Rev. Lett.* **48**, 1559 (1982)
 - ⁵ M.A. Zudov, R.R. Du, J.A. Simmons, and J.R. Reno, *Phys. Rev. B* **64**, 201311(R) (2001).
 - ⁶ P.D. Ye, L.W. Engel, D.C. Tsui, J.A. Simmons, J.R. Wendt, G.A. Vawter, J.L. Reno, *Appl. Phys. Lett.* **79**, 2193 (2001).
 - ⁷ R. Mani, J.H. Smet, K. von Klitzing, V. Narayanamurti, W.B. Johnson, and V. Umansky, *Nature* **420**, 646 (2002).
 - ⁸ M.A. Zudov, R.R. Du, L.N. Pfeiffer, K.W. West, *Phys. Rev. Lett.* **90**, 046807 (2003).
 - ⁹ A.V. Andreev, I.L. Aleiner, A.J. Millis, *Phys. Rev. Lett.* **91**, 056803 (2003).
 - ¹⁰ I.A. Dmitriev, A.D. Mirlin, D.G. Polyakov, M.A. Zudov, *Rev. Mod. Phys.* **84**, 1709 (2012).
 - ¹¹ V. I. Ryzhii, *Fiz. Tverd. Tela* **11**, 2577 (1969) [*Sov. Phys. Solid State* **11**, 2078 (1970)].
 - ¹² A.C. Durst, S. Sachdev, N. Read, and S.M. Girvin, *Phys. Rev. Lett.* **91**, 086803 (2003).
 - ¹³ I.A. Dmitriev, A.D. Mirlin, and D.G. Polyakov, *Phys. Rev. Lett.* **91**, 226802 (2003).
 - ¹⁴ D. Konstantinov and K. Kono, *Phys. Rev. Lett.* **103**, 266808 (2009).
 - ¹⁵ D. Konstantinov and K. Kono, *Phys. Rev. Lett.* **105**, 226801 (2010).
 - ¹⁶ M.E. Raikh and T.V. Shahbazyan, *Phys. Rev. B* **49**, 5531 (1994).
 - ¹⁷ T.H. Sander, S.N. Holmes, and J.J. Harris, *Phys. Rev.* **58**, 13856 (1998).
 - ¹⁸ Yu.P. Monarkha, *Fiz. Nizk. Temp.* **37**, 108 (2011) [*Low Temp. Phys.* **37**, 90 (2011)].
 - ¹⁹ Yu.P. Monarkha, *Fiz. Nizk. Temp.* **37**, 829 (2011) [*Low Temp. Phys.* **37**, 655 (2011)].
 - ²⁰ Yu.P. Monarkha, *Fiz. Nizk. Temp.* **38**, 579 (2012) [*Low Temp. Phys.* **38**, 451 (2012)].
 - ²¹ D. Konstantinov, A. Chepelianskii, and K. Kono, *J. Phys. Soc. Jpn.* **81**, 093601 (2012).
 - ²² D. Konstantinov, M. Watanabe, and K. Kono, *J. Phys. Soc. Jpn.* **82**, 075002 (2013).
 - ²³ A.D. Chepelianskii, M. Watanabe, K. Nasyedkin, K. Kono, D. Konstantinov, *Nature Communications* **6**, 7210 (2015).
 - ²⁴ Yu.P. Monarkha, *Fiz. Nizk. Temp.* **42**, 567 (2016) [*Low Temp. Phys.* **42**, 441 (2016)].
 - ²⁵ D. Konstantinov, Yu. Monarkha, K. Kono, *Phys. Rev. Lett.* **111**, 266802 (2013).
 - ²⁶ C.C. Grimes and G. Adams, *Phys. Rev. Lett.* **42**, 795 (1979).
 - ²⁷ F.M. Peeters, and P.M. Platzman, *Phys. Rev. Lett.* **50**, 2021 (1983).
 - ²⁸ G. Bastard, *Wave mechanics applied to semiconductor heterostructures*, EDP Sciences, Les Ulis Cedex, France (1992).
 - ²⁹ J.H. Davies, *The physics of low-dimensional semiconductors*, Cambridge University Press, Cambridge (1998).
 - ³⁰ H.L. Stormer A.C. Gossard W. Wiegmann, *Solid State Comm.* **41**, 707 (1982).
 - ³¹ J. J. Harris, D. E. Lacklinton, C.T. Foxon, F. M. Selten, A. M. Suckling, R. J. Nicholas, and K. W. J. Barnham, *Semicond. Sci. Technol.* **2**, 783 (1987).
 - ³² T. Ando and Y. Uemura, *J. Phys. Soc. Jpn.* **36**, 959 (1974).
 - ³³ R. Kubo, H. Hasegawa, N. Hashitsume, *Journ. Phys. Soc. Japan* **14**, 56 (1959).
 - ³⁴ R. Kubo, S.J. Miyake, and N. Hashitsume, *Solid State Phys.* **17**, 269 (1965).
 - ³⁵ Yu.P. Monarkha, *Fiz. Nizk. Temp.* **39**, 1068 (2013) [*Low Temp. Phys.* **39**, 828 (2013)].
 - ³⁶ X.L. Lei, C.S.Ting, *Phys. Rev. B* **30**, 4809 (1984).
 - ³⁷ W. Cai, X.L. Lei, C.S. Ting, *Phys. Rev. B* **31**, 4070 (1985).
 - ³⁸ Yu.P. Monarkha, E. Teske, and P. Wyder, *Phys. Rep.* **370**, 1 (2002).
 - ³⁹ Yu.P. Monarkha and K. Kono, *Two-Dimensional Coulomb Liquids and Solids*, Springer-Verlag, Berlin, Heidelberg (2004).
 - ⁴⁰ S. Titeica, *Ann. Physik* [5] **22**, 129 (1935).
 - ⁴¹ P.J.M. Peters, P. Scheuzger, M.J. Lea, Yu.P. Monarkha, P.K.H. Sommerfeld, and R.W. van der Heijden, *Phys. Rev. B* **50**, 11570 (1994).
 - ⁴² Yu.P. Monarkha, *Fiz. Nizk. Temp.* **43**, 819 (2017) [*Low Temp. Phys.* **43**, 650 (2017)].
 - ⁴³ Yu. Monarkha and D. Konstantinov, *J. Low Temp. Phys.* **197**, 208 (2019).
 - ⁴⁴ R.R. Gerhardts, *Surf. Sci.* **58**, 227 (1976).
 - ⁴⁵ T. Ando, *J. Phys. Soc. Jpn.* **37**, 622 (1974).
 - ⁴⁶ E. Adams, T. Holstein, *Journ. Phys. Chem. Solids* **10**, 254 (1959).

- ⁴⁷ In the online version of the AIP publishing paper [*Low Temp. Phys.* **46**, 569 (2020)], in spite of the efforts of the author it was impossible to avoid the responsible person's ability to destroy Eq. (23). In the original online version of *Fiz. Nizk. Temp.* **46**, 682 (2020), this equation is correct.
- ⁴⁸ G.D. Mahan, *Many-Particle Physics*, 3rd edn. Kluwer Academic/Plenum Publishers, New York, Boston, Dordrecht, London (2000).
- ⁴⁹ W. Zawadzki and R. Lassnig, *Surface Sci.* **142**, 225 (1984).
- ⁵⁰ D. Konstantinov, H. Isshiki, Yu. Monarkha, H. Akimoto, K. Shirahama, K. Kono, *Phys. Rev. Lett.* **98**, 235302 (2007).